

Editor's Summary

Is the Cause of Hydrocephalus Blood Simple?

Hydrocephalus or "water on the brain" is caused by accumulation of cerebrospinal fluid (CSF) in the cerebral ventricles during fetal development and is one of the most common neurological disorders of newborns, occurring in 1 in 1500 live births. One apparent cause of hydrocephalus is bleeding into the cerebral ventricles or brain tissue of the fetus, suggesting that factors or components in blood may trigger development of this severe neurological disorder. The most common treatment is surgical insertion of an intraventricular shunt that drains excess CSF from the cerebral ventricles, but this approach only relieves intracranial pressure and does not solve the root cause of the disorder. Yung *et al.* set out to investigate which factors in blood trigger hydrocephalus using an in vivo fetal mouse model that they developed. They identify a blood-borne lipid called lysophosphatidic acid (LPA) as a potential cause of hydrocephalus and show that when LPA is prevented from binding to its receptor LPA₁ by a receptor antagonist, that hydrocephalus does not develop in fetal mice.

The authors injected serum, plasma, or red blood cells into the cerebral ventricles of the brains of fetal mice in utero at 13.5 days of gestation. The animals were then assessed prenatally 1 or 5 days later or postnatally at several different time points. Injection of serum or plasma but not red blood cells induced CSF accumulation and hydrocephalus, with animals displaying enlarged heads, dilated ventricles, and thinning of the cortex. The investigators reasoned that LPA, a blood-borne lipid that is known to be important for the developing cerebral cortex, might be involved in the development of hydrocephalus. When they injected a solution containing LPA into the cerebral ventricles of fetal mice in utero, the mice did indeed develop severe hydrocephalus. The authors wondered how an increase in LPA might affect cortical development and lead to hydrocephalus. They show that injection of LPA resulted in altered adhesion and mislocalization of neural progenitor cells along the surface of the ventricles and that this mislocalization depended on expression of the LPA₁ receptor by these cells. When the researchers repeated their experiments with fetal mice lacking the LPA₁ receptor, they were unable to induce hydrocephalus. The key finding came with their demonstration that an LPA₁ receptor antagonist blocked the ability of LPA to induce hydrocephalus in the fetal mice. These results suggest that LPA and its LPA₁ receptor may be new therapeutic targets for developing drugs that could be used in conjunction with surgery to treat this debilitating neurological disease.

A complete electronic version of this article and other services, including high-resolution figures, can be found at:

<http://stm.sciencemag.org/content/3/99/99ra87.full.html>

Supplementary Material can be found in the online version of this article at:

<http://stm.sciencemag.org/content/suppl/2011/09/02/3.99.99ra87.DC1.html>

Related Resources for this article can be found online at: <http://stm.sciencemag.org/content>

Information about obtaining **reprints** of this article or about obtaining **permission to reproduce this article** in whole or in part can be found at:

<http://www.sciencemag.org/about/permissions.dtl>

HYDROCEPHALUS

Lysophosphatidic Acid Signaling May Initiate Fetal Hydrocephalus

Yun C. Yung,^{1,2} Tetsuji Mutoh,^{1*} Mu-En Lin,^{1,2} Kyoko Noguchi,¹ Richard R. Rivera,¹ Ji Woong Choi,^{1†} Marcy A. Kingsbury,^{1‡} Jerold Chun^{1§}

Fetal hydrocephalus (FH), characterized by the accumulation of cerebrospinal fluid, an enlarged head, and neurological dysfunction, is one of the most common neurological disorders of newborns. Although the etiology of FH remains unclear, it is associated with intracranial hemorrhage. Here, we report that lysophosphatidic acid (LPA), a blood-borne lipid that activates signaling through heterotrimeric guanosine 5'-triphosphate-binding protein (G protein)-coupled receptors, provides a molecular explanation for FH associated with hemorrhage. A mouse model of intracranial hemorrhage in which the brains of mouse embryos were exposed to blood or LPA resulted in development of FH. FH development was dependent on the expression of the LPA₁ receptor by neural progenitor cells. Administration of an LPA₁ receptor antagonist blocked development of FH. These findings implicate the LPA signaling pathway in the etiology of FH and suggest new potential targets for developing new treatments for FH.

INTRODUCTION

Fetal hydrocephalus (FH) is a life-threatening condition resulting from excessive accumulation of cerebrospinal fluid (CSF) that occurs in 1 in 1500 newborns annually (1). FH is treated by palliative shunt placement or ventriculostomy to drain excess fluid from the brain; other neurosurgical and pharmacological interventions have proven suboptimal (2). There is some evidence for genetic contributions to rare forms of hydrocephalus, but most cases are sporadic with an unclear etiology (3).

Intriguing observations have linked FH to prenatal bleeding events, such as intracranial or germinal matrix hemorrhage, which could produce pathophysiological exposure to blood derivatives like plasma and serum (1). This suggests that factors associated with blood could contribute to FH (2). Furthermore, FH has been associated with alterations in neural cell fate in the cerebral cortex, suggesting that intracranial hemorrhage and FH may share a common pathogenic process (3). A molecule found in blood and the developing cerebral cortex is the lipid lysophosphatidic acid (LPA). LPA is produced through multiple biochemical pathways (4) and has numerous biological properties that are mediated through a family of six known heterotrimeric guanosine 5'-triphosphate-binding protein (G protein)-coupled receptors, LPA₁ to LPA₆ (5, 6). LPA is also a normal component of blood and blood derivatives such as plasma and serum. Human serum may have LPA concentrations exceeding 30 μ M during clotting (4); this is from 5000- to more than 15,000-fold the EC₅₀ (median effective concentration) of its receptors as measured in neural progenitor cell assays (7). Multiple LPA receptors are expressed in the embryonic cerebral cortex (8). LPA receptor-dependent signaling influences a broad range of cellular processes that can alter the electrophysiological, cytoskeletal, morphological, antiapoptotic, and proliferative properties of neural

progenitor cells (5). Neural progenitor cells, such as radial glia, divide and give rise to postmitotic neural cells that form the mature cerebral cortex. Additionally, radial glia generate the ciliated ependymal cells that line the surface of the ventricles in the brain. LPA receptor-dependent effects can thus alter the overall organization of the embryonic cortex (9, 10).

To assess whether exposure of the embryonic brain to prenatal blood, serum, or LPA may be implicated in FH, we developed an embryonic mouse model of FH. In this model, the brains of mouse embryos were exposed to blood components or to LPA and were analyzed pre- and postnatally for development of FH. We further investigated the role of LPA and its cognate receptor LPA₁ in the induction of FH and were able to block FH development in our model using a small molecule that inhibits LPA₁ receptor signaling.

RESULTS

Serum or plasma exposure induces FH

Intracranial hemorrhage and blood clotting can expose the developing brain to a combination of red blood cells (RBCs), plasma, or serum. In our study, these components were isolated and delivered intraventricularly to the cerebral cortex of mouse embryos at embryonic day 13.5 (E13.5) (Fig. 1, A to C). In this mouse model of FH, pregnant animals underwent laparotomy in which the uterine horns were accessed and the embryos were visualized by direct illumination. Solutions were delivered through the uterine wall and fetal cranium into the lateral ventricles (LVs) of the fetal brain as a single bolus dose. The mice were analyzed at different stages of fetal development and postnatally for the development of FH. Fetal delivery of serum or plasma induced development of FH, with postnatal animals displaying characteristic dome-shaped, enlarged heads, dilated LVs, and thinning of the cortex (Fig. 1, E and H). Cohorts exposed prenatally to serum or plasma developed hydrocephalus in 25 and 50% of animals (Fig. 1N; $n = 12$ and $n = 6$, respectively), whereas uninjected animals or those exposed to vehicle or injection of RBCs did not (Fig. 1, D, G, and N; $n = 19$). In addition, early cortical wall disruption appeared in wild-type animals after 24 hours of exposure to serum or plasma but not to

¹Dorris Neuroscience Center, The Scripps Research Institute, La Jolla, CA 92037, USA.

²Biomedical Sciences Program, University of California at San Diego School of Medicine, La Jolla, CA 92093, USA.

*Present address: Gunma Kokusai Academy, 1361-4 Uchigashima-cho, Ota, Gunma 373-0813, Japan.

†Present address: Department of Pharmacology, College of Pharmacy, Gachon University of Medicine and Science, Incheon 406-799, Korea.

‡Present address: Department of Biology, Indiana University, Bloomington, IN 47401, USA.

§To whom correspondence should be addressed. E-mail: jchun@scripps.edu

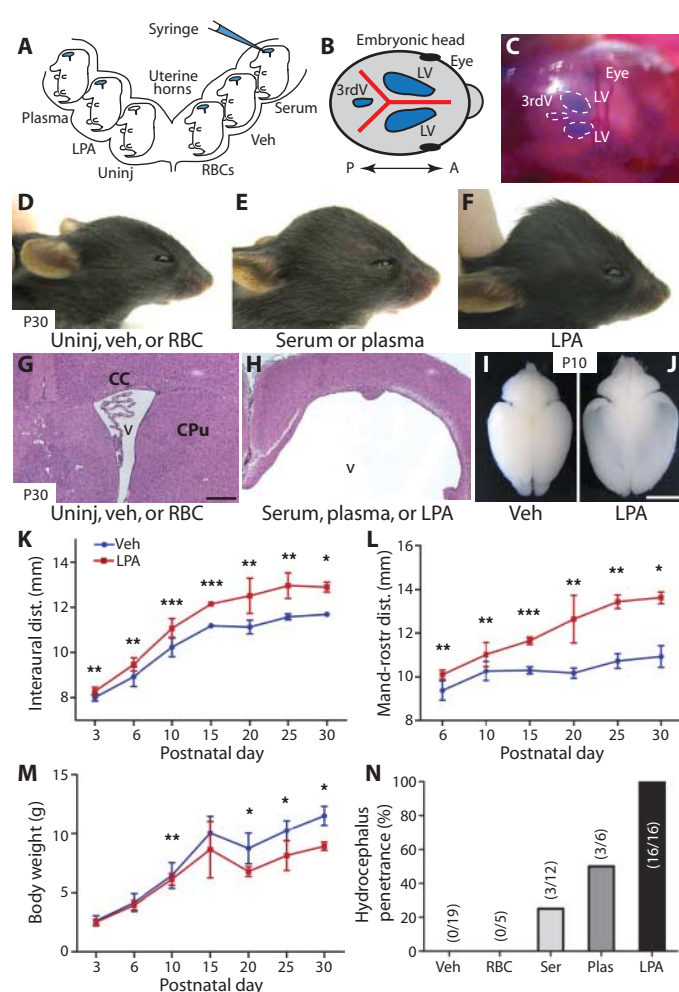


Fig. 1. Induction of hydrocephalus in mouse embryos exposed to plasma, serum, or LPA. **(A)** Diagram of in utero injections. Pregnant dams underwent laparotomy, the E13.5 embryos were visualized by direct illumination, and 3- μ l solutions of vehicle, plasma, serum, RBCs, or LPA were injected into the cerebral cortex of individual embryos. The dams were sutured and embryos were examined after 1 day (E14.5), 5 days (E18.5), or postnatally at P4, P10, P21, and 4 weeks. **(B and C)** Visualization (blue) of lateral ventricles (LV) and third ventricles (3rdV), indicating diffusion of injected material. Blue dye was mixed with the injection solutions so that accurate targeting of the LVs could be monitored. The presence of blue color in all ventricles indicated cerebroventricular patency. A, anterior; P, posterior. **(D to F)** Mice at postnatal day 30 (P30) developed macrocephalic heads after injection of plasma, serum, or LPA, but not after injection of vehicle or RBCs. **(G and H)** Histological examination of these injected mice (P30) showed grossly dilated ventricles (v) and thinning of the overlying cerebral cortex. CC, corpus callosum; CPu, caudate and putamen. **(I and J)** Whole-brain preparations from mice at P10 comparing control- and LPA-injected cortex; note the increased dimensions and transparency characteristic of hydrocephalus in the LPA-injected mice (J). **(K to M)** Animals exposed to LPA ($n = 7$) (red) showed increased head dimensions and decreased body weight compared to vehicle control ($n = 10$) (blue) (average \pm SD; * $P \leq 0.05$, ** $P \leq 0.01$, *** $P \leq 0.001$, Mann-Whitney test; see table S3 for P values). **(N)** Hydrocephalus penetrance was quantified for each exposure condition; numbers in parentheses represent the number of hydrocephalic animals/cohort. Scale bars, 400 μ m [(G) and (H)] and 0.5 cm [(I) and (J)].

RBCs (fig. S1, A to F). These data indicated that hydrocephalus could be initiated by hemorrhagic components, which is consistent with epidemiological data (1) and an animal model of intracranial bleeding that reported the development of ventricular dilation and hydrocephalus (11). These data also demonstrated that neither RBCs nor an acute increase in ventricular fluid volume produced by vehicle injection was sufficient to produce sustained ventricular dilation or FH (Fig. 1, D and N). This supports the possibility that a serum or plasma factor or factors are capable of initiating hydrocephalus.

LPA exposure induces histological changes and FH

LPA is a bioactive factor present in both plasma and serum that can alter the organization of the embryonic cerebral cortex ex vivo (9), and its activities might contribute to the induction of FH. The effects of embryonic LPA exposure were examined in wild-type embryos at E13.5, an age when neural progenitor cells respond robustly to LPA (7, 9), and at later developmental ages. Markedly, LPA-injected animals developed severe hydrocephalus 100% of the time (Fig. 1, F, H, and N; $n = 16$) that was clearly visible by postnatal day 10 (P10) based on ventricular dilation and cortical thinning (Fig. 1, H and J). Hydrocephalus was not observed in vehicle-injected ($n = 19$) or noninjected littermates ($n = 10$) (Fig. 1, D, G, I, and N). Hydrocephalic animals showed progressively increasing head width (interaural distance, Fig. 1K), head height (mandibular-rostral distance, Fig. 1L), and body weight loss (Fig. 1M), although there was no significant difference in the anterior-posterior dimension (fronto-occipital distance) (fig. S3A). In addition, these hydrocephalic animals displayed dome-shaped heads (Fig. 1F) and altered subcortical structures such as caudate, putamen, and corpus callosum (Fig. 1H). Hydrocephalic animals survived from 2 to 6 weeks after birth (fig. S3B).

Histological alterations found in mouse models and clinical cases of human hydrocephalus (table S1) were observed after exposure to LPA, but not vehicle control. Lateral ventricular size was bilaterally increased after LPA exposure compared to vehicle control (Fig. 2, A to C, and fig. S4, A to L). In addition, the apical ventricular surface (which comprises neural progenitor cells at this age) was disrupted and showed protrusions into the LVs (Fig. 2, D to F). In severely disrupted areas, rounded cell clusters appeared to detach from the ventricular surface (Fig. 2, G to I). These clusters were immunoreactive for nestin (a neural progenitor cell marker), incorporated bromodeoxyuridine (BrdU), and expressed *Lpar1* detected by in situ hybridization (fig. S5, A to I). *Lpar1* expression is present in the ventricular zone (VZ) of the brain, confirming that the clusters were of VZ origin. Furthermore, the formation of neurospheres—abnormal, radially oriented cells—within the VZ was observed (Fig. 2, J to L). Finally, other areas of the cerebroventricular system were also affected, for example, the third ventricle, another CSF-filled cavity located caudal and medial to the LVs. Cells from the third ventricular wall protruded into the CSF-filled ventricle, consistent with partial third ventricle occlusion (Fig. 2, M to Q). This abnormal localization of cells (heterotopia) is consistent with heterotopia observed in FH patients (12). One mechanism that could contribute to these diverse pathological findings is altered adhesion of neural progenitor cells induced by LPA signaling that may result in abnormal cell migration and positioning in the fetal mouse brain (13).

LPA exposure disrupts neural progenitor cell function

Cell adhesion molecules required for the formation of adherens junctions between cells help to maintain the luminal integrity of the cere-

broventricular system. Knockout or knockdown of various molecular components that maintain ventricular integrity such as N-cadherin (14, 15), Celsr 2 and 3 (cadherin EGF LAG seven-pass G-type receptor

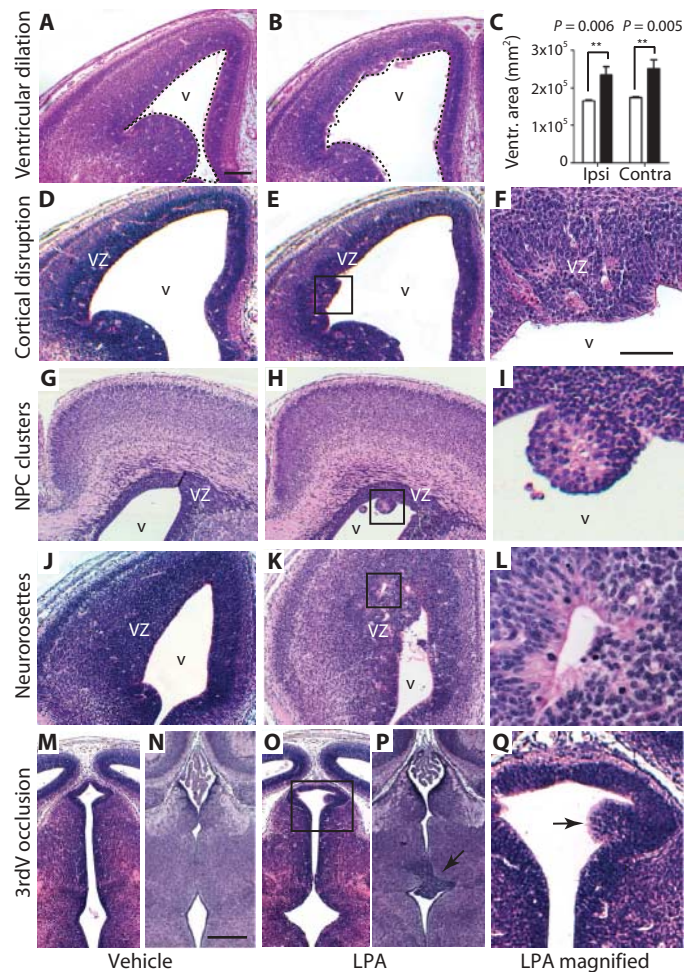


Fig. 2. Exposure of mouse embryos to LPA induces FH. (A to Q) Data from mouse embryos cortically injected at embryonic day 13.5 (E13.5) with LPA (B, E, F, H, I, K, L, O, P, and Q) (magnified in F, I, L, and Q) or vehicle control (A, D, G, J, M, and N). (A to C) Ventricular dilation. Embryos injected with LPA (analyzed at E14.5) showed dilation of the LVs compared to embryos injected with vehicle (dotted outlines indicate ventricles), with changes quantified in (C) ($n = 3$ embryos per condition; average \pm SD; $P = 0.006$, $P = 0.005$, unpaired t test; Ipsi, ipsilateral; Contra, contralateral). (D to F) Cortical disruption. LPA exposure (analyzed at E14.5) produced cortical disruption of ventricular zone (VZ) organization and protrusions of neural progenitor cells along the apical ventricular surface [boxed area magnified in (F)]. (G to I) Neural progenitor cell clusters in the LVs. Clusters of neural progenitor cells (NPC) protrude from the apical VZ surface and can be found as isolated clusters throughout the ventricle (analyzed at E18.5). (J to L) Neurospheres. These LPA-induced structures are composed of radially oriented neural progenitor cells located throughout the VZ. (M to Q) Partial occlusion of the third ventricle. Disruption of the third ventricular wall, associated with partial ventricular occlusion, was observed [analyzed at E14.5 in (M), (O), and (Q), see arrow, or at E18.5 in (N) and (P)]. Scale bars, 200 μ m [(A), (B), (D), (E), (G), (H), (J), (K), (M), (N), (O), and (P)] and 50 μ m [(F), (I), (L), and (Q)].

types 2 and 3) (16), myosin II-B (17), myosin IXa (18), Lgl1 (lethal giant larvae 1) (19), and Dlg5 (discs, large homolog 5) (20) produces histological features found in human hydrocephalus (table S1). LPA has been shown to both increase and decrease cell-cell contacts mediated by N-cadherin in a cell type- and receptor subtype-specific manner (13, 21). This suggests that modulation of LPA signaling may affect the integrity of the brain's ventricles. The apical surface of the LVs was examined for N-cadherin expression that was found to be discontinuous in LPA-exposed mouse embryos but not vehicle control-treated embryos (Fig. 3, A and B). Consistent with N-cadherin's function in maintaining the correct attachment of dividing neural progenitor cells to the apical surface (15), LPA-injected embryos showed a marked increase in the incorrect upward and basal positioning of mitotic cells (Fig. 3, C, D, and I; $P = 0.002$, unpaired t test). In addition, clusters of neural progenitor cell spheres (Fig. 2, H and I) (29 ± 7.1 per LPA-exposed embryo) were observed floating within the ventricles of LPA-treated embryos. This is consistent with the finding of neural progenitor cells in the CSF of newborns with post-hemorrhagic hydrocephalus (22).

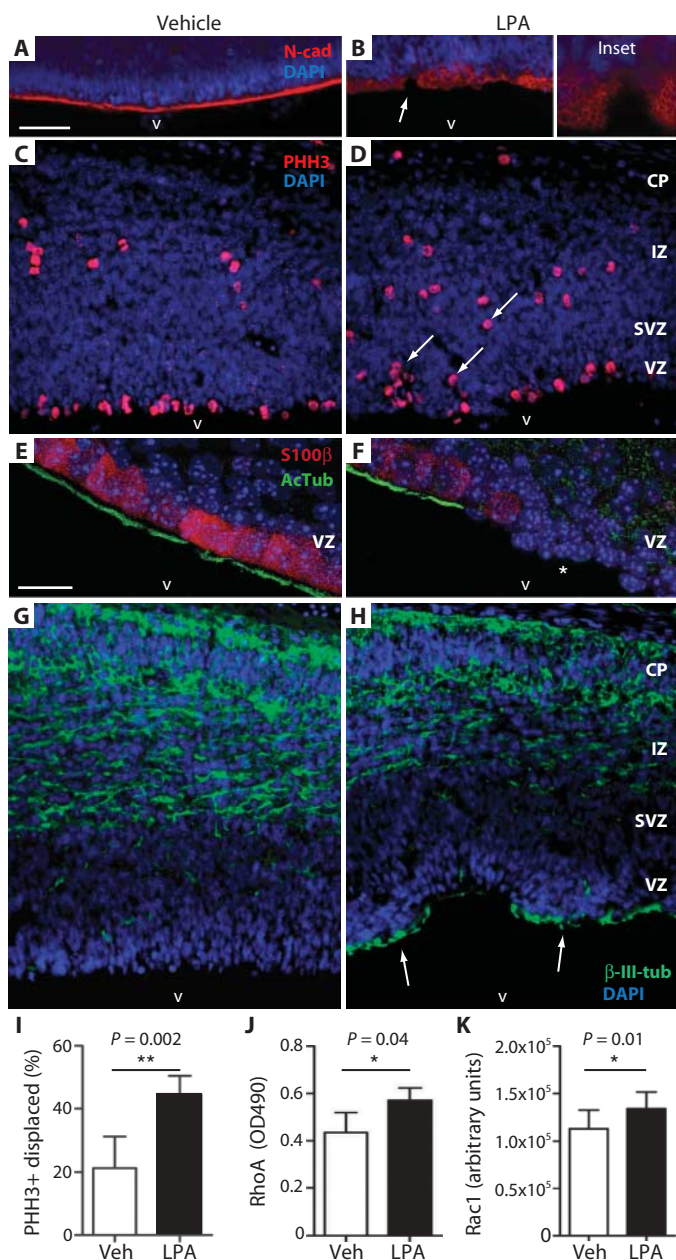
A cause of hydrocephalus is loss of cilia or ciliary function on the ependymal cells lining the ventricular surface, where the cilia are thought to reduce the flow of CSF along the ventricle walls (23–30). Ependymal cells differentiate during mid to late neurogenesis in the developing brain and mature in early postnatal life to form a single multiciliated cell layer that can be identified by immunostaining for S100 β and acetylated α -tubulin (31). After exposure of mouse embryos to LPA, alterations in ependymal cells were observed at P4. Partial loss of mature ependymal cells, identified by the co-absence of S100 β and acetylated α -tubulin immunoreactivities, manifested as discrete regions lacking cells (Fig. 3, E and F, and videos S1 and S2). These results are consistent with the reported loss, or denudation, of ependymal cells in both clinical cases and mouse models of FH (25, 29).

LPA activates Rho and Rac in the embryonic cortex

LPA receptors, particularly LPA₁, are powerful activators of the small guanosine triphosphatase (GTPase) Rho (32), as well as the closely related GTPase Rac (33). To determine the possible involvement of these pathways in LPA-induced FH, we examined Rho and Rac signaling using ex vivo cerebral cortical cultures grown in the presence or absence of LPA, followed by measurements using an enzyme-linked immunosorbent assay (ELISA). There was activation of both prototypical members RhoA ($n = 6$ pairs; $P = 0.04$, paired t test) and Rac1 ($n = 6$ pairs; $P = 0.01$, paired t test) in the embryonic cortex (7) after LPA stimulation (Fig. 3, J and K, and fig. S6, A to C). These results confirm the activation of both Rho and Rac by LPA signaling in the mouse embryonic cerebral cortex under conditions that could promote FH.

Serum, plasma, and LPA induce LPA receptor-dependent FH

Several blood-related factors such as transforming growth factor- β (TGF- β) and vascular endothelial growth factor (VEGF) have been reported to be elevated in CSF from hydrocephalic individuals (34). When administered to young mice, these growth factors can cause ventricular dilation and hydrocephalus (35). This raised the possibility that factors in addition to LPA, present in plasma and serum, could be responsible for producing FH and associated histological changes



observed in this mouse model. To address this question, we injected mouse embryos having genetic deletion of specific LPA receptors with plasma, serum, or LPA and then assessed them pre- and postnatally. Based on gene expression studies, LPA₁ and LPA₂ receptors were expressed in the neural progenitor cell population of the VZ (figs. S7, A to L, and S8, A and B) and are coupled to the same G proteins that mediate LPA signaling (9, 36). To minimize receptor compensation, we examined LPA₁ and LPA₂ double-null mutant mice (LPA₁^{-/-} LPA₂^{-/-}) together with LPA₂ homozygous null/LPA₁ heterozygote (LPA₁^{+/-} LPA₂^{-/-}) mice. Both LPA₁^{-/-} LPA₂^{-/-} and LPA₁^{+/-} LPA₂^{-/-} mouse embryos were exposed to plasma, serum, or LPA. These analyses revealed that exposure to these agents in LPA₁^{+/-} LPA₂^{-/-} mice produced results

Fig. 3. Cell and molecular effects of LPA exposure. Exposure of mouse embryos to LPA resulted in displacement of mitotic neural progenitor cells resulting in their mislocalization and activation of Rho/Rac signaling. (**A** and **B**) Exposure to LPA, but not vehicle (analyzed at E14.5), disrupted the apical ventricular surface and altered N-cadherin (N-cad) expression (red; arrow magnified in inset). Cell nuclei are counterstained with DAPI (blue). (**C** and **D**) The displacement of mitotic neural progenitor cells was identified by immunolabeling phosphorylated histone H3 (PHH3+, red). Displaced mitotic cells are abnormally positioned superficially in the VZ and SVZ (D, arrows; LPA-treated) rather than along the ventricular surface as in (C) (vehicle-treated). CP, cortical plate; IZ, intermediate zone; SVZ, subventricular zone. (**E** and **F**) Immunolabeled ependymal cells of the VZ (S100β+, red) show loss of their cilia (AcTub+, green) after LPA exposure (F) compared to vehicle controls (E) when analyzed at P4. LPA exposure decreased the number of S100β+ ependymal cells, resulting in loss of cilia from the ventricular surface (asterisk, F). (**G** and **H**) Postmitotic neurons identified by immunolabeling with β-III-tubulin (β-III-tub+, green) indicated VZ disruption in regions of the cortex exposed to LPA and the presence of heterotopic neurons (H, arrows) compared to vehicle control (G). (**I**) Quantification of mitotically displaced neural progenitor cells identified by PHH3 immunolabeling ($n = 5$ embryos per condition; average \pm SD; ** $P = 0.0022$, unpaired t test). (**J** and **K**) Quantification of RhoA and Rac1 activation in ex vivo mouse embryonic cortex after exposure to LPA or vehicle for 3 min. Ex vivo culture involved dissection and removal of whole cortical hemispheres from E13.5 embryos for culture in cell media with timed exposure to either condition. RhoA: $n = 5$ pairs of matched cortical hemispheres exposed to vehicle or 10 μ M LPA; average \pm SD; * $P = 0.0408$, paired t test. Rac1: $n = 6$ pairs of matched cortical hemispheres exposed to vehicle or 10 μ M LPA; average \pm SD; * $P = 0.01$, paired t test. Scale bars, 50 μ m [(A) to (D), (G), and (H)] and 20 μ m [(E) and (F)].

indistinguishable from those of wild-type controls, indicating a primary role for the LPA₁ receptor in the induction of FH (Fig. 4, A to K, fig. S9, A to G, and tables S2 and S3). Both wild-type and LPA₁^{+/-} LPA₂^{-/-} mice were subsequently used as controls and compared to double-null mutant animals. Both plasma and serum induced cortical disruption that was abrogated in double-null mutant mice (fig. S1, A, B, D, and E). Critically, LPA's ability to induce FH and associated histological changes (tables S1 and S2) was strongly dependent on the expression of LPA₁. In LPA₁^{+/-} LPA₂^{-/-} control animals exposed to LPA, FH showed complete penetrance ($n = 10$, 100%). In contrast, FH was reduced to about 10% in double-null mutant mice ($n = 9$, 11%) (Fig. 4K, fig. S9, A to G, and table S1). The rare occurrence of FH in double-null mutant animals likely reflects contributions by one or more of the remaining four LPA receptors rescuing the double-null phenotype. These data suggest that FH, along with associated histological changes, induced by plasma, serum, or LPA exposure, is primarily dependent on the LPA₁ receptor.

Pharmacological LPA₁ blockade prevents FH and histological changes

The identification of LPA receptor signaling as a potential initiating cause of FH suggested that pharmacological modulation of LPA receptors could influence the development of FH. Ki16425, a receptor antagonist with proven specificity against LPA₁ and LPA₃ (37), was intraventricularly injected before LPA exposure. Available genetic and expression data did not support a role for LPA₃ in LPA-induced FH (38, 39). Mouse embryos that were treated with vehicle followed by

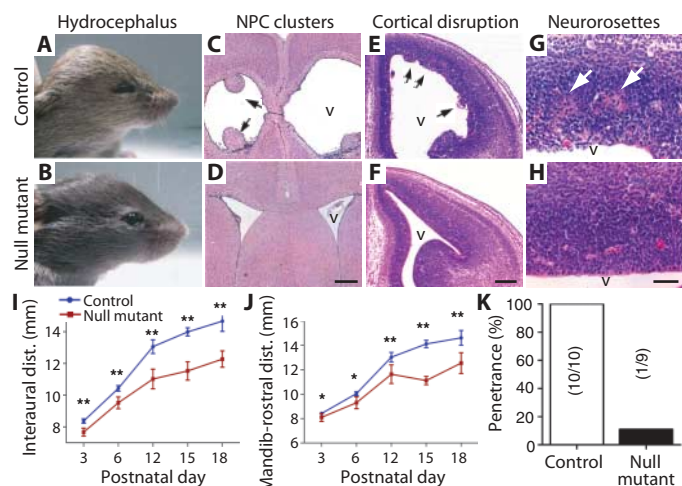


Fig. 4. LPA does not induce hydrocephalus in LPA_1/LPA_2 receptor double-null mice. (A and B) Head dilation and hydrocephalus are observed in postnatal animals after LPA exposure at E13.5 in control ($LPA_1^{+/+} LPA_2^{-/-}$) (A) but not double-null mutant mice ($LPA_1^{-/-} LPA_2^{-/-}$) (B). (C to H) LPA-injected positive control animals showed neural progenitor cell clusters (C, arrows), early cortical disruption at E14.5 (E, arrowheads), and neurorosettes (G, arrows); these were generally absent [see (K)] in double-null mutant mice exposed to LPA (D, F, and H). (I and J) LPA exposure in control mice ($n = 10$, blue line) revealed increased interaural (I) and mandibular-rostral distance (J) as early as P3 that was attenuated in the double-null mutant animals ($n = 9$, red line) (see Fig. 1, wild-type LPA exposure) ($n \geq 3$ embryos per genotype; average \pm SD; $P < 0.05$, unpaired t test; see table S3). (K) Penetrance of LPA-induced hydrocephalus was quantified; numbers in parentheses represent number of hydrocephalic animals/total cohort. Scale bars, 400 μ m [(C) and (D)], 200 μ m [(E) and (F)], and 50 μ m [(G) and (H)].

LPA showed similar cortical defects compared to mice treated with LPA only ($n = 5$) (Fig. 5, A and B). In contrast, mouse embryos treated with Ki16425 followed by LPA showed a marked reduction in FH and related histological changes ($n = 5$) (Fig. 5, C, D, and G to I). In the control, treatment with Ki16425 followed by vehicle produced no such effects ($n = 4$) (Fig. 5, E to I). These data demonstrate that pharmacological intervention targeting LPA receptors, particularly LPA_1 , could attenuate development of LPA-induced FH. These pharmacological studies on wild-type mice independently support the results obtained with the receptor-null mice and also eliminate the possibility that constitutive receptor deletion produces developmental artifacts that somehow prevent FH.

DISCUSSION

Here, we generated a new mouse model of FH through exposure of the brains of mouse embryos to blood components or the bioactive lipid LPA. Using this model, we showed that the histological consequences of FH occurred mainly through the LPA_1 receptor signaling pathway in neural progenitor cells within the developing cerebral cortex and that these effects could be blocked by either genetic deletion or pharmacological inhibition of this G protein-coupled receptor. We propose that LPA_1 receptor signaling is a molecular mechanism that

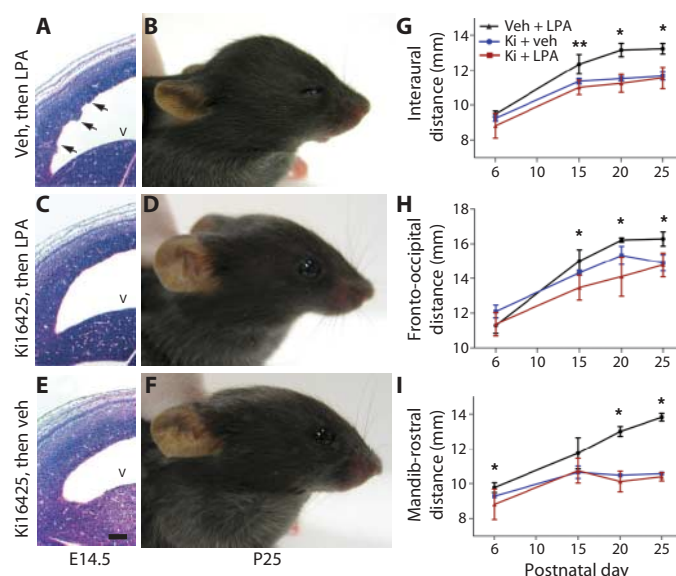


Fig. 5. Hydrocephalus can be blocked by an LPA_1 receptor antagonist. (A and B) Mouse embryos were injected sequentially with vehicle followed by LPA 10 min later at E13.5 and were examined at E14.5 (A) or were assessed for hydrocephalus postnatally (B, P25). (C and D) Pharmacological intervention with the Ki16425 (Ki) antagonist of LPA_1 and LPA_3 receptors was assessed in the same way but replacing vehicle with Ki16425 followed by LPA, and then analyzing the animals during embryonic development (C) and postnatally (D). (E and F) The effects of antagonist alone were assessed with Ki16425 followed by vehicle, and then embryonic and postnatal assessment for hydrocephalus. Apical protrusions of ventricular cell clusters (A, arrows) were observed 24 hours later in embryos injected with vehicle and then LPA but not in embryos injected with drug and then LPA, or drug then vehicle (C and E). Scale bar, 100 μ m. (G to I) Quantitative assessments measured head dimensions in positive controls and animals exposed to drug. Positive controls (animals exposed to vehicle then LPA) showed the expected changes in head dimensions and hydrocephalus (black lines, G to I). In each set of head dimension measurements, statistically significant increases were observed in vehicle + LPA-treated mice compared with the normal head measurements obtained with drug + LPA-treated animals (red and blue lines, G to I). No statistically significant changes were observed between drug and vehicle (blue line)-injected and drug and LPA (red line)-injected embryos ($n \geq 3$ embryos per condition; average \pm SD; $P > 0.05$, unpaired t test; see table S3).

may account for the epidemiological observations linking prenatal bleeding and FH (Fig. 6). Intracranial hemorrhage into the germinal matrix (or VZ layer) of the developing cerebral cortex and into CSF results in abnormally high concentrations of LPA that aberrantly activate LPA_1 receptors expressed by neural progenitor cells. This in turn activates downstream intracellular signaling components to produce disorganization and thinning of cortical layers and ultimately FH (Fig. 6). Additional histological consequences of aberrant LPA_1 receptor activation include neural progenitor cell cluster formation, third ventricle occlusion, and loss of cilia along the lateral ventricular walls. How these changes relate precisely to each other remains to be determined. Additional endpoints such as CSF overproduction and elevated intracranial pressure remain to be tested in this model, particularly as they relate to

Development of fetal hydrocephalus

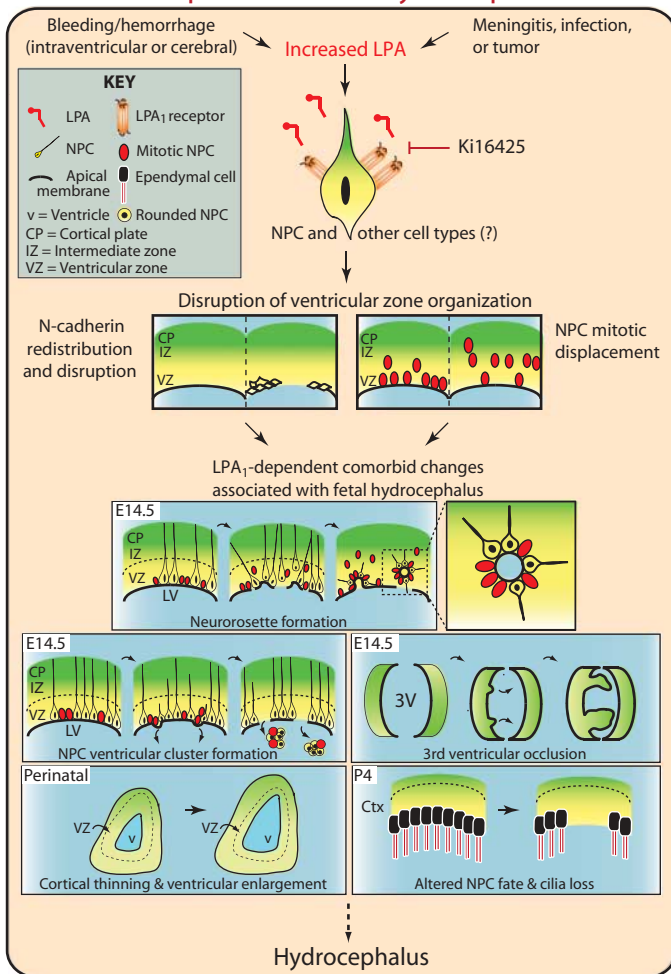


Fig. 6. Model for how LPA could induce FH. Intraventricular hemorrhage may lead to an increase in the concentration of LPA in the brain, resulting in aberrant activation of LPA₁ receptors on neural progenitor cells with concomitant activation of downstream G protein signaling components such as the GTPases Rho and Rac. The ensuing disruption of adherens junctions between neural progenitor cells results in their displacement in the VZ. Subsequent pathological alterations include neurorosette formation and formation of neural progenitor cells into ventricular clusters. This results in occlusion of the third ventricle, cortical thinning, ventricular enlargement, and altered neural progenitor cell fate and loss, which together result in FH. Pharmacological blockade of LPA₁ receptor signaling using the LPA₁ receptor antagonist Ki16425 prevents aberrant activation of this signaling cascade in response to LPA and abrogates development of FH.

these histological changes. Aberrant activation of LPA receptors may explain the diverse histological presentation reported for human FH, and is consistent with other FH-relevant animal models (table S1). Based on genetic and pharmacological studies, the primary receptor mediating these effects is LPA₁ with comparatively minor contributions by other LPA receptor subtypes. Although other contributory factors in addition to LPA may be present in blood, genetic deletion of LPA

receptors prevented plasma and serum from inducing FH. This suggests a primary role for receptor-mediated LPA signaling in the development of FH.

A variety of gene mutations in animals have been reported to result in FH. LPA signaling has been documented to interface with many of these genes and their activated pathways. FH has been linked to cadherins (15, 20), adhesion molecules that are altered by LPA signaling (40). Loss of myosin IIB and IXa results in hydrocephalus, consistent with participation of myosin pathways in the developing central nervous system (CNS) and their modulation by LPA signaling (41). The small GTPase Rho that is activated by LPA (13, 36) has also been linked to FH (18). We showed that this signaling component, along with its partner Rac, was activated in the cerebral cortex of mouse embryos exposed to LPA. Through its presence in blood, LPA thus has the potential to modulate one or more molecular pathways that have been linked to FH.

Genetic deletions in cilia-related proteins, such as Polaris (Tg737), Stumpy, or Hydin (24, 26, 27, 30), or mutations leading to primary ciliary dyskinesia (42), have been implicated in FH, suggesting that loss of cilia may contribute to the development of this disorder. The loss of cilia observed in the current study, which appears to result from disruption of neural progenitor cells, is consistent with altered cell fate whereby ciliated ependymal cells are reduced due to death of neural progenitor cells or their differentiation into nonciliated cell types (29). This phenomenon of ciliary loss complements previous genetic data and connects the action of LPA (through pathological exposure of the cerebral cortex to blood) to dysfunction of neural progenitor cells and loss of ciliated ependymal cells in FH.

In previous work, aberrant activation of LPA signaling in ex vivo organotypic cerebral cortical cultures of fetal brain produced major disruption of neural progenitor cell function and gross disorganization of the cortex including abnormal cortical folding resembling polygyrations (9). This ex vivo method relied on the dissection, separation, and culture of intact cortical hemispheres in the continuous presence of LPA. However, the limited survival time of the cultures (~20 hours) prevented multiday and prenatal versus postnatal comparisons. In contrast, we were able to recapitulate ventricular dilation and other histological changes observed in human FH using our in vivo model of FH reported here (9). Both in vivo and ex vivo data implicate displacement of neural progenitor cells as a causative factor in FH (Fig. 3) (9). Contrasting effects observed between the in vivo and the ex vivo studies can be explained by the existence of additional elements such as growth factors and cytokines in our in vivo system that are known to influence neurogenesis and formation of the cerebral cortex (43, 44). Blockage of CSF flow (which was not duplicated in ex vivo cultures) may also contribute to FH (45). Other differences between the in vivo and ex vivo studies include localized ventricular administration of a single bolus of LPA versus whole-brain exposure to LPA, respectively. Despite these differences, the acute disruption of mitotic neural progenitor cells and the dependence of this disruption on the LPA₁ receptor were conserved between the in vivo and ex vivo studies. Intriguingly, some hydrocephalic patients have also been reported to exhibit cortical polygyrations, consistent with the effects seen during prolonged ex vivo cortical exposure to LPA (46).

The cellular alterations that resulted in dilated ventricles, neurorosettes, ventricular disruption and occlusion, and cilia loss are likely due to the direct effects of LPA receptor activation on neural progenitor cells in the VZ rather than on secondary effects that result from

hemorrhage or the actions of other factors in blood. First, intraventricular exposure to plasma or serum can induce FH in some but not all exposed mouse embryos. However, FH was absent in $LPA_1^{-/-}$ $LPA_2^{-/-}$ double-null mice, indicating that non-LPA blood products, if present, played a minor role in inducing FH. Second, at the age that mouse embryos were exposed to LPA (E13.5), the LPA_1 receptor is expressed primarily by neural progenitor cells in the VZ (fig. S7, A to L) (7). The observed histological defects were inconsistent with primary disruption involving the diffuse organization of blood vessels throughout the cerebral cortical wall (38, 47), which should have produced effects throughout the cortex and noncortical neuraxis where blood vessels are also present. The LPA_1 receptor is also expressed in the superficial marginal zone (future layer 1 of the cortex) and developing meninges at E13.5 (fig. S7, E, G, and I), leaving open possible contributions to FH by the cells in these regions. Third, pharmacological antagonism of the LPA_1 receptor prevented LPA-induced FH. This result eliminates the possibility that developmental perturbations of neural progenitor cells or blood vessels induced by loss of $LPA_1^{-/-}$ and $LPA_2^{-/-}$ prevented the development of FH. The precise roles of individual LPA receptor subtypes on defined cells in FH remain to be determined.

Several potential limitations of this *in vivo* model should be mentioned. First, the progression of cortical brain development in mice is similar but not identical to the extended course in humans. Second, the spatiotemporal extent of intracranial hemorrhage and severity of exposure to blood in fetuses is not well delineated; thus, this bolus exposure model likely only approximates the spectrum of pathological insults during development of human FH. Future translational studies focused on patient samples may help to refine this animal model. Although this study focused on a preventative strategy in which the LPA_1 receptor antagonist was delivered before LPA exposure, there was likely to be considerable temporal overlap between exposure of the mouse embryonic brain to both LPA and antagonist. Furthermore, we note that neural progenitor cell loss and ventricular dilation occurred prenatally but progressed to severe hydrocephalus only at neonatal ages, indicating that FH progression may occur in stages, as reported in humans (25). This underscores the feasibility of a therapeutic strategy whereby early prenatal ventricular dilation associated with intracranial hemorrhage could be ameliorated by short-term LPA receptor modulators without affecting LPA-mediated normal cortical development but reducing or preventing hydrocephalus.

The identification of LPA signaling in the initiation of FH is consistent with a diverse range of reported risk factors that share FH as a common endpoint. Reported risk factors include bleeding, hypoxia, infection, meningitis, and brain tumors, all of which have been associated with increased LPA signaling (48–51). The disparate histological phenomena associated with human FH (table S1) can be reproduced by exposure of embryonic mouse brain to LPA, supporting a shared molecular mechanism in both mice and humans. The ability to prevent FH by pharmacologically blocking LPA signaling suggests that LPA and its LPA_1 receptor have potential as therapeutic targets for treating at least some forms of FH. Whether other forms of FH are amenable to this treatment strategy requires further study. Finally, it is notable that a host of developmentally linked disorders including cerebral palsy (52), schizophrenia (53), and autism (54) have also been epidemiologically associated with prenatal bleeding, suggesting that future studies should investigate a potential connection between aberrant LPA signaling and these neurodevelopmental disorders.

MATERIALS AND METHODS

Injection solutions

LPA (18:1) (Avanti Polar Lipids) solution [10 and 20 mM in Hanks' balanced salt solution (HBSS)] was prepared fresh just before use by ultrasonication in a water bath (Branson) for 15 min at 22°C. Whole blood was obtained from female adult mice by cardiac puncture collection and clotted for 1 hour on ice. The clot was manually removed, and the remaining solution was spun down at 2000 rpm for 20 min at 4°C. The top "serum" and bottom "red blood cell" (washed and resuspended in HBSS) fractions were collected by centrifugation separation. The "plasma" fraction was obtained as previously described (11). Ki16425 (Kirin Brewery, 1 mM final concentration in HBSS) was prepared for intraventricular injections. BrdU solution was prepared (Sigma, 100 mg/kg final concentration) for intraperitoneal injection.

Injections

All procedures followed proper animal use and care guidelines that were approved by the Institutional Animal Care and Use Committee at The Scripps Research Institute. *In utero* injections of 3 μ l of vehicle (HBSS), plasma, serum, RBC, or LPA solutions into embryonic cortices were performed on pentobarbital anesthetized (Nembutal, 50 mg/kg), timed-pregnant dams at E13.5. Embryos were examined after 1 day (E14.5), 5 days (E18.5), or postnatally at P4, P10, P21, and 4 weeks. For Ki16425 intervention experiments, E13.5 embryonic cortices were injected with 1.5 μ l of Ki16425, exposed for 15 min, and then subsequently injected ipsilaterally with 1.5 μ l of LPA solution (20 mM), sutured, and examined 1 day later. For postnatal assessment, pups were allowed to be birthed naturally. Because uterine positional order was lost during delivery, all embryos within each litter were injected with identical ligands. Pharmacological studies were performed with 1.5 μ l of each ligand (LPA at double concentration) to maintain consistent injection volumes across studies.

Histology

Pregnant dams were intraperitoneally anesthetized with pentobarbital (50 mg/kg), during which the embryos were collected whole by surgical dissection, decapitated, and heads fixed in formalin–alcohol–acetic acid solution (FAA) or 4% paraformaldehyde (PFA). Subsequently, the anesthetized dams were killed by cervical dislocation. Naturally birthed pups were anesthetized with pentobarbital and transcardially perfused with FAA or PFA. Their brains were immersion-fixed with FAA or PFA, paraffinized with an automated processor (Sakura), and embedded in paraffin. The tissue was sectioned (6- to 10- μ m thickness), dewaxed, and stained with hematoxylin and eosin. Only healthy embryos with observable heartbeats were analyzed ($\geq 95\%$ injected).

Immunofluorescence

Brains preserved in FAA or PFA were examined. Sucrose cryoprotected/frozen heads fixed in PFA were sectioned (16 μ m), blocked with species-appropriate serum, and immunolabeled. Paraffin sections (6 to 10 μ m) were additionally dewaxed and processed through sodium citrate buffer (10 mM, 0.05% Tween 20, pH 6.0) antigen retrieval before antibody staining. Antibodies specific for the following antigens were used in overnight staining at 4°C: nestin (BD Biosciences, mouse, 1:400), β -III-tubulin (Covance, mouse, 1:1000), phosphorylated histone H3 (Ser¹⁰) (Millipore, rabbit, 1:1000), S100 β (Abcam, rabbit, 1:500),

acetylated α -tubulin (Sigma, mouse, 1:1000), N-cadherin (Calbiochem, rabbit, 1:200), and BrdU (Roche, rat, 1:50). Mouse-, rabbit-, or rat-specific secondary antibodies conjugated with Alexa Fluor 488 or Cy3 (Invitrogen or Jackson ImmunoResearch, donkey, 1:1000) were used for visualization. Nuclei were counterstained with 4',6-diamidino-2-phenylindole (DAPI, Sigma).

Image acquisition and quantification

Epifluorescence images were acquired on a Zeiss Imager 1D microscope (AxioVision 4.7.2 software) with appropriate fluorescence filters. Confocal images were acquired on an Olympus FluoView 500 laser scanning microscope with appropriate lasers and optimized Z steps, sequential channel acquisition, and Kalman filtering of 4. Confocal image stacks were analyzed and reconstructed into videos with MetaMorph software (version 7, Molecular Devices). Images and manual counting were analyzed by investigators blinded as to sample identity. Inadvertent loss of blinding occurred when differences between control and experimental samples were markedly obvious but would not have altered the basic interpretation and results of this study. Photoshop adjustments (version 11.0, Adobe) were strictly limited to light level and contrast enhancement for visual aesthetics that did not change data interpretation.

Statistical analysis

Statistical analyses were performed with Prism software (version 5, GraphPad). Normality of data distribution was tested with the *F* test for unequal variance. Normally distributed data were analyzed with unpaired or paired Student's *t* test when comparing between two data groups. Nonnormally distributed data were analyzed with the nonparametric Mann-Whitney test and Kruskal-Wallis and Dunnett's post hoc tests when comparing between two and three data groups, respectively. Data were expressed as average \pm SD and considered significant if tests indicated $P \leq 0.05$.

Head size measurement

Increased head circumference, clinically used as a standard indicator of hydrocephalus, is typically measured with a cloth tape above the ears, but is not technically feasible nor accurately reproducible in early postnatal mice because of small size and incomplete skull calcification. Instead, an electronic caliper (C-master digital gauge) was used to perform three unidimensional measurements: interaural distance (ear to ear), mandibular-rostral distance (jaw to top of the head), and fronto-occipital distance (forehead to back of the head). Individual measurements were performed in triplicate and averaged. Measurements were performed at P3, P6, P10, P12, P15, P18, P20, P25, and P30. Postnatal animals were tattooed for individual identification.

Ventricle area measurement

Paraffinized embryo heads in coronal presentation were serially cut (10- μ m thickness). Sections at 100- μ m intervals from anterior to posterior were imaged. LVs were manually traced, and area sizes were calculated automatically with AxioVision software (version 4.7.2, Carl Zeiss) and tabulated. At least six sections were measured per embryo.

Construction and labeling of in situ hybridization probes

Mouse *Lpar1* exon 3 was amplified by polymerase chain reaction (PCR) from a bacterial artificial chromosome (BAC) template with

Pfx50 DNA polymerase (Invitrogen) with the following primers: A1Ex3For, 5'-TTCACAGCCATGAACGAACAAC-3' and A1Ex3Rev, 5'-ACCAAGCACAATGACCACAGTC-3', and tailed with Taq polymerase. The 748-base pair product was then isolated with the QIAEX II DNA isolation kit (Qiagen), cloned into the pGem-T Easy T vector (Promega), and linearized with appropriate restriction enzymes. Digoxigenin (DIG)-labeled sense and antisense runoff transcripts were transcribed with DIG labeling mix (Roche) and SP6 and T7 RNA polymerases (Roche), respectively. DIG-labeled sense and antisense mouse *Lpar2* probes were prepared as previously described (38).

In situ hybridization

Embryo heads were examined for *Lpar1* and *Lpar2* expression as previously described (7). Paraffin sections were dewaxed and rehydrated with diethyl pyrocarbonate (DEPC)-treated solutions before hybridization. All probes were hybridized at 65°C.

RhoA and Rac1 activation ELISA assay

Fresh embryonic cortical hemispheres were dissected out in ice-cold Opti-MEM (Invitrogen). Matched hemispheres were cultured in media supplemented with 10 μ M LPA and 0.1% fatty acid-free bovine serum albumin or without LPA, essentially as previously described (9, 55). LPA stimulation was terminated in ice-cold Opti-MEM without LPA. The cortical wall was dissected away from the ganglionic eminences, triturated in lysis buffer, and snap-frozen in liquid nitrogen. Activation of RhoA and Rac1 was measured with absorbance- or chemiluminescence-based G-LISA kits, respectively, according to the manufacturer's instructions (Cytoskeleton) with an EL800 microplate reader and a SynergyMX luminometer (Bio-Tek). Antibody concentrations were optimized for machine sensitivity. Statistically significant but modest activation levels likely reflect the absence of serum starvation, used to approximate in vivo conditions, along with the influence of other endogenous signaling pathways that increase the basal activation of Rho and Rac.

LPA measurements

The LPA extraction method was adapted with some modification (56). Briefly, 50 μ l of tissue homogenate [final concentration (fresh tissue) 200 to 400 mg/ml] was used for each sample. Methanol/HCl (187.5 μ l, 10:1 mixture) and 625 μ l of methyl-*tert*-butyl ether (MTBE) were added to each sample and incubated on a nutator at 22°C for 1 hour. Distilled water (157 μ l) was then added to the mixture, incubated for 10 min, and phase-separated by centrifugation at 13,000 rpm for 10 min. The initial organic phase was collected, whereas the aqueous phase was reextracted with 250 μ l of MTBE/methanol/H₂O (10:3:2.5 ratio). Both organic phases were combined and dried with a SpeedVac concentrator (Savant) and resuspended in 100 μ l of methanol. Non-natural 17:0 LPA (Avanti Polar Lipids) was added as an internal standard. The extracts were subjected to liquid chromatography-mass spectrometry (LC-MS) for LPA measurement at the TSRI Mass Spectrometry Core with an Agilent 6410 triple quad mass spectrometer coupled to an Agilent 1200lc stack. Compounds were eluted with a mobile phase of H₂O/ACN 90:10 with 10 mM NH₄OAc (A) and ACN/H₂O with 10 mM NH₄OAc (B) at 0.2 ml/min. Agilent 300SB-C8 2.1 mm \times 100 mm, 3.5 μ m columns were used. The gradient was $t = 0$, 80:20 (A/B); $t = 5$, 50:50; $t = 7$, 25:75; $t = 15$, 0:100; $t = 20$, off. There was a 5-min re-equilibration time between samples. The source was maintained at 350°C with a drying gas flow of 10 liters/hour, and data were collected in negative ion mode. The following transition states were monitored:

18:1 LPA mass/charge ratio (m/z) ratio, 435→153; 17:0 LPA m/z ratio, 423→153. Calibration curves were generated with 10 to 10,000 fmol per injection of 18:0 LPA. Peak areas of [M-H] for LPA (18:1) form were normalized to the internal standard and plotted versus concentration.

SUPPLEMENTARY MATERIAL

www.sciencetranslationalmedicine.org/cgi/content/full/3/99/99ra87/DC1

Fig. S1. Serum and plasma but not RBCs produce LPA receptor-dependent cortical wall disruption.

Fig. S2. Experimental parameters of LPA cortical exposure model.

Fig. S3. Lack of fronto-occipital changes and survival curve of LPA-injected animals that develop hydrocephalus over time.

Fig. S4. Bilaterally increased ventricular area and mitotic displacement following LPA exposure.

Fig. S5. LPA exposure induces the formation of denuded cell clusters that originate from the ventricular zone of the developing cortex.

Fig. S6. LPA induces RhoA and Rac1 activation.

Fig. S7. Expression of *Lpar1* in the developing embryonic brain at E13.5.

Fig. S8. Expression of *Lpar2* in the developing embryonic brain at E13.5.

Fig. S9. LPA-induced cortical disruption and mitotic displacement are abrogated in double-null mutant mice.

Table S1. Shared pathological features of hydrocephalus in FH patients and mouse models.

Table S2. Histological features associated with hydrocephalus are abrogated in LPA₁ and LPA₂ double-null animals.

Table S3. Average ± SD, n , and P values of data graphed in Figs. 1, 4, and 5.

References

Descriptions for Videos S1 and S2

Video S1. Ciliated ependymal cells are maintained at the apical ventricular surface after vehicle exposure.

Video S2. Ciliated ependymal cells are lost in an incomplete fashion at the apical ventricular surface after LPA exposure.

REFERENCES AND NOTES

1. E. K. Persson, S. Anderson, L. M. Wiklund, P. Uvebrant, Hydrocephalus in children born in 1999–2002: Epidemiology, outcome and ophthalmological findings. *Childs Nerv. Syst.* **23**, 1111–1118 (2007).
2. D. Shooman, H. Portess, O. Sparrow, A review of the current treatment methods for post-haemorrhagic hydrocephalus of infants. *Cerebrospinal Fluid Res.* **6**, 1 (2009).
3. J. Zhang, M. A. Williams, D. Rigamonti, Genetics of human hydrocephalus. *J. Neurol.* **253**, 1255–1266 (2006).
4. J. Aoki, A. Taira, Y. Takanezawa, Y. Kishi, K. Hama, T. Kishimoto, K. Mizuno, K. Saku, R. Taguchi, H. Arai, Serum lysophosphatidic acid is produced through diverse phospholipase pathways. *J. Biol. Chem.* **277**, 48737–48744 (2002).
5. J. W. Choi, D. R. Herr, K. Noguchi, Y. C. Yung, C. W. Lee, T. Mutoh, M. E. Lin, S. T. Teo, K. E. Park, A. N. Mosley, J. Chun, LPA receptors: Subtypes and biological actions. *Annu. Rev. Pharmacol. Toxicol.* **50**, 157–186 (2010).
6. K. Yanagida, K. Masago, H. Nakanishi, Y. Kihara, F. Hamano, Y. Tajima, R. Taguchi, T. Shimizu, S. Ishii, Identification and characterization of a novel lysophosphatidic acid receptor, p2y5/LPA6. *J. Biol. Chem.* **284**, 17731–17741 (2009).
7. J. H. Hecht, J. A. Weiner, S. R. Post, J. Chun, *Ventricular zone gene-1 (vzg-1)* encodes a lysophosphatidic acid receptor expressed in neurogenic regions of the developing cerebral cortex. *J. Cell Biol.* **135**, 1071–1083 (1996).
8. K. Noguchi, D. Herr, T. Mutoh, J. Chun, Lysophosphatidic acid (LPA) and its receptors. *Curr. Opin. Pharmacol.* **9**, 15–23 (2009).
9. M. A. Kingsbury, S. K. Rehen, J. J. Contos, C. M. Higgins, J. Chun, Non-proliferative effects of lysophosphatidic acid enhance cortical growth and folding. *Nat. Neurosci.* **6**, 1292–1299 (2003).
10. G. Estivill-Torrús, P. Llebregz-Zayas, E. Matas-Rico, L. Santín, C. Pedraza, I. De Diego, I. Del Arco, P. Fernández-Llebregz, J. Chun, F. R. De Fonseca, Absence of LPA₁ signaling results in defective cortical development. *Cereb. Cortex* **18**, 938–950 (2008).
11. S. S. Cherian, S. Love, I. A. Silver, H. J. Porter, A. G. Whitelaw, M. Thoresen, Posthemorrhagic ventricular dilation in the neonate: Development and characterization of a rat model. *J. Neuropathol. Exp. Neurol.* **62**, 292–303 (2003).
12. V. L. Sheen, L. Basel-Vanagaite, J. R. Goodman, I. E. Scheffer, A. Bodell, V. S. Ganesh, R. Ravenscroft, R. S. Hill, T. J. Cherry, Y. Y. Shugart, J. Barkovich, R. Straussberg, C. A. Walsh, Etiological heterogeneity of familial periventricular heterotopia and hydrocephalus. *Brain Dev.* **26**, 326–334 (2004).
13. J. A. Weiner, N. Fukushima, J. J. Contos, S. S. Scherer, J. Chun, Regulation of Schwann cell morphology and adhesion by receptor-mediated lysophosphatidic acid signaling. *J. Neurosci.* **21**, 7069–7078 (2001).
14. S. I. Gänzler-Odenthal, C. Redies, Blocking N-cadherin function disrupts the epithelial structure of differentiating neural tissue in the embryonic chicken brain. *J. Neurosci.* **18**, 5415–5425 (1998).
15. M. Kadowaki, S. Nakamura, O. Machon, S. Krauss, G. L. Radice, M. Takeichi, N-cadherin mediates cortical organization in the mouse brain. *Dev. Biol.* **304**, 22–33 (2007).
16. F. Tissir, Y. Qu, M. Montcouquiol, L. Zhou, K. Komatsu, D. Shi, T. Fujimori, J. Labeau, D. Tyteca, P. Courtoy, Y. Poumay, T. Uemura, A. M. Goffinet, Lack of cadherins *Celsr2* and *Celsr3* impairs ependymal ciliogenesis, leading to fatal hydrocephalus. *Nat. Neurosci.* **13**, 700–707 (2010).
17. X. Ma, J. Bao, R. S. Adelstein, Loss of cell adhesion causes hydrocephalus in nonmuscle myosin II-B-ablated and mutated mice. *Mol. Biol. Cell* **18**, 2305–2312 (2007).
18. M. Abouhamed, K. Grobe, I. V. San, S. Thelen, U. Honnert, M. S. Balda, K. Matter, M. Bähler, Myosin IXa regulates epithelial differentiation and its deficiency results in hydrocephalus. *Mol. Biol. Cell* **20**, 5074–5085 (2009).
19. O. Klezovitch, T. E. Fernandez, S. J. Tapscott, V. Vasioukhin, Loss of cell polarity causes severe brain dysplasia in *Lgl1* knockout mice. *Genes Dev.* **18**, 559–571 (2004).
20. T. Nechiporuk, T. E. Fernandez, V. Vasioukhin, Failure of epithelial tube maintenance causes hydrocephalus and renal cysts in *Dlg5*^{-/-} mice. *Dev. Cell* **13**, 338–350 (2007).
21. K. Yanagida, S. Ishii, F. Hamano, K. Noguchi, T. Shimizu, LPA₄/p2y9/GPR23 mediates Rho-dependent morphological changes in a rat neuronal cell line. *J. Biol. Chem.* **282**, 5814–5824 (2007).
22. R. C. Krueger Jr., H. Wu, M. Zandian, M. Danielpour, P. Kabos, J. S. Yu, Y. E. Sun, Neural progenitors populate the cerebrospinal fluid of preterm patients with hydrocephalus. *J. Pediatr.* **148**, 337–340 (2006).
23. M. Fukumizu, S. Takashima, L. E. Becker, Neonatal posthemorrhagic hydrocephalus: Neuropathologic and immunohistochemical studies. *Pediatr. Neurol.* **13**, 230–234 (1995).
24. B. Banizs, M. M. Pike, C. L. Millican, W. B. Ferguson, P. Komlosi, J. Sheetz, P. D. Bell, E. M. Schwiebert, B. K. Yoder, Dysfunctional cilia lead to altered ependyma and choroid plexus function, and result in the formation of hydrocephalus. *Development* **132**, 5329–5339 (2005).
25. M. D. Domínguez-Pinos, P. Páez, A. J. Jiménez, B. Weil, M. A. Arráez, J. M. Pérez-Figares, E. M. Rodríguez, Ependymal denudation and alterations of the subventricular zone occur in human fetuses with a moderate communicating hydrocephalus. *J. Neuropathol. Exp. Neurol.* **64**, 595–604 (2005).
26. H. R. Dawe, M. K. Shaw, H. Farr, K. Gull, The hydrocephalus inducing gene product, *Hydin*, positions axonemal central pair microtubules. *BMC Biol.* **5**, 33 (2007).
27. T. Town, J. J. Breunig, M. R. Sarkisian, C. Spilianakis, A. E. Ayoub, X. Liu, A. F. Ferrandino, A. R. Gallagher, M. O. Li, P. Rakic, R. A. Flavell, The *stumpy* gene is required for mammalian ciliogenesis. *Proc. Natl. Acad. Sci. U.S.A.* **105**, 2853–2858 (2008).
28. C. Wodarczyk, I. Rowe, M. Chiaravalli, M. Pema, F. Qian, A. Boletta, A novel mouse model reveals that polycystin-1 deficiency in ependyma and choroid plexus results in dysfunctional cilia and hydrocephalus. *PLoS One* **4**, e7137 (2009).
29. P. Páez, L. F. Bätz, R. Roales-Buján, L. M. Rodríguez-Pérez, S. Rodríguez, A. J. Jiménez, E. M. Rodríguez, J. M. Pérez-Figares, Patterned neuropathologic events occurring in hyh congenital hydrocephalic mutant mice. *J. Neuropathol. Exp. Neurol.* **66**, 1082–1092 (2007).
30. K. F. Lechtreck, P. Delmotte, M. L. Robinson, M. J. Sanderson, G. B. Witman, Mutations in *Hydin* impair ciliary motility in mice. *J. Cell Biol.* **180**, 633–643 (2008).
31. N. Spassky, F. T. Merkle, N. Flames, A. D. Tramontin, J. M. Garcia-Verdugo, A. Alvarez-Buylla, Adult ependymal cells are postmitotic and are derived from radial glial cells during embryogenesis. *J. Neurosci.* **25**, 10–18 (2005).
32. A. J. Ridley, A. Hall, The small GTP-binding protein rho regulates the assembly of focal adhesions and actin stress fibers in response to growth factors. *Cell* **70**, 389–399 (1992).
33. F. N. Van Leeuwen, C. Olivo, S. Grivell, B. N. Giepmans, J. G. Collard, W. H. Moolenaar, Rac activation by lysophosphatidic acid LPA₁ receptors through the guanine nucleotide exchange factor Tiam1. *J. Biol. Chem.* **278**, 400–406 (2003).
34. A. Heep, B. Stoffel-Wagner, P. Bartmann, S. Benseler, C. Schaller, P. Groneck, M. Obladen, U. Felderhoff-Mueser, Vascular endothelial growth factor and transforming growth factor-β1 are highly expressed in the cerebrospinal fluid of premature infants with post-hemorrhagic hydrocephalus. *Pediatr. Res.* **56**, 768–774 (2004).
35. S. Cherian, M. Thoresen, I. A. Silver, A. Whitelaw, S. Love, Transforming growth factor-βs in a rat model of neonatal posthaemorrhagic hydrocephalus. *Neuropathol. Appl. Neurobiol.* **30**, 585–600 (2004).
36. I. Ishii, J. J. Contos, N. Fukushima, J. Chun, Functional comparisons of the lysophosphatidic acid receptors, LP_{A1}/VZG-1/EDG-2, LP_{A2}/EDG-4, and LP_{A3}/EDG-7 in neuronal cell lines using a retrovirus expression system. *Mol. Pharmacol.* **58**, 895–902 (2000).

37. H. Ohta, K. Sato, N. Murata, A. Damirin, E. Malchinkhuu, J. Kon, T. Kimura, M. Tobo, Y. Yamazaki, T. Watanabe, M. Yagi, M. Sato, R. Suzuki, H. Murooka, T. Sakai, T. Nishitoba, D. S. Im, H. Nochi, K. Tamoto, H. Tomura, F. Okajima, Ki16425, a subtype-selective antagonist for EDG-family lysophosphatidic acid receptors. *Mol. Pharmacol.* **64**, 994–1005 (2003).
38. C. McGiffert, J. J. Contos, B. Friedman, J. Chun, Embryonic brain expression analysis of lysophospholipid receptor genes suggests roles for *s1p₁* in neurogenesis and *s1p₁₋₃* in angiogenesis. *FEBS Lett.* **531**, 103–108 (2002).
39. A. E. Dubin, D. R. Herr, J. Chun, Diversity of lysophosphatidic acid receptor-mediated intracellular calcium signaling in early cortical neurogenesis. *J. Neurosci.* **30**, 7300–7309 (2010).
40. J. Jourquin, N. Yang, Y. Kam, C. Guess, V. Quaranta, Dispersal of epithelial cancer cell colonies by lysophosphatidic acid (LPA). *J. Cell. Physiol.* **206**, 337–346 (2006).
41. N. Fukushima, Y. Morita, Actomyosin-dependent microtubule rearrangement in lysophosphatidic acid-induced neurite remodeling of young cortical neurons. *Brain Res.* **1094**, 65–75 (2006).
42. I. Ibañez-Tallon, A. Pagenstecher, M. Fliegau, H. Olbrich, A. Kispert, U. P. Ketelsen, A. North, N. Heintz, H. Omran, Dysfunction of axonemal dynein heavy chain *Mdnah5* inhibits ependymal flow and reveals a novel mechanism for *hydrocephalus* formation. *Hum. Mol. Genet.* **13**, 2133–2141 (2004).
43. J. A. Miyan, M. Zendah, F. Mashayekhi, P. J. Owen-Lynch, Cerebrospinal fluid supports viability and proliferation of cortical cells in vitro, mirroring in vivo development. *Cerebrospinal Fluid Res.* **3**, 2 (2006).
44. A. Gato, M. E. Desmond, Why the embryo still matters: CSF and the neuroepithelium as interdependent regulators of embryonic brain growth, morphogenesis and histogenesis. *Dev. Biol.* **327**, 263–272 (2009).
45. P. J. Owen-Lynch, C. E. Draper, F. Mashayekhi, C. M. Bannister, J. A. Miyan, Defective cell cycle control underlies abnormal cortical development in the hydrocephalic Texas rat. *Brain* **126**, 623–631 (2003).
46. P. Humphreys, D. P. Muzumdar, L. E. Sly, J. Michaud, Focal cerebral mantle disruption in fetal hydrocephalus. *Pediatr. Neurol.* **36**, 236–243 (2007).
47. D. Stubbs, J. DeProto, K. Nie, C. Englund, I. Mahmud, R. Hevner, Z. Molnár, Neurovascular congruence during cerebral cortical development. *Cereb. Cortex* **19** (Suppl. 1), i32–i41 (2009).
48. W. R. Wikoff, G. Pendyala, G. Siuzdak, H. S. Fox, Metabolomic analysis of the cerebrospinal fluid reveals changes in phospholipase expression in the CNS of SIV-infected macaques. *J. Clin. Invest.* **118**, 2661–2669 (2008).
49. K. J. Herr, D. R. Herr, C. W. Lee, K. Noguchi, J. Chun, Stereotyped fetal brain disorganization is induced by hypoxia and requires lysophosphatidic acid receptor 1 (LPA1) signaling. *Proc. Natl. Acad. Sci. U.S.A.* 10.1073/pnas.1106129108 (2011).
50. K. R. Baumforth, J. R. Flavell, G. M. Reynolds, G. Davies, T. R. Pettit, W. Wei, S. Morgan, T. Stankovic, Y. Kishi, H. Arai, M. Nowakova, G. Pratt, J. Aoki, M. J. Wakelam, L. S. Young, P. G. Murray, Induction of autotaxin by the Epstein-Barr virus promotes the growth and survival of Hodgkin lymphoma cells. *Blood* **106**, 2138–2146 (2005).
51. Y. Kishi, S. Okudaira, M. Tanaka, K. Hama, D. Shida, J. Kitayama, T. Yamori, J. Aoki, T. Fujimaki, H. Arai, Autotaxin is overexpressed in glioblastoma multiforme and contributes to cell motility of glioblastoma by converting lysophosphatidylcholine to lysophosphatidic acid. *J. Biol. Chem.* **281**, 17492–17500 (2006).
52. M. Vukojević, I. Soldo, D. Granić, Risk factors associated with cerebral palsy in newborns. *Coll. Antropol.* **33** (Suppl. 2), 199–201 (2009).
53. C. M. Hultman, P. Sparén, N. Takei, R. M. Murray, S. Cnattingius, Prenatal and perinatal risk factors for schizophrenia, affective psychosis, and reactive psychosis of early onset: Case-control study. *BMJ* **318**, 421–426 (1999).
54. A. Kolevzon, R. Gross, A. Reichenberg, Prenatal and perinatal risk factors for autism: A review and integration of findings. *Arch. Pediatr. Adolesc. Med.* **161**, 326–333 (2007).
55. S. K. Rehen, M. A. Kingsbury, B. S. Almeida, D. R. Herr, S. Peterson, J. Chun, A new method of embryonic culture for assessing global changes in brain organization. *J. Neurosci. Methods* **158**, 100–108 (2006).
56. V. Matyash, G. Liebisch, T. V. Kurzchalia, A. Shevchenko, D. Schwudke, Lipid extraction by methyl-*tert*-butyl ether for high-throughput lipidomics. *J. Lipid Res.* **49**, 1137–1146 (2008).
57. **Acknowledgments:** We thank G. Kennedy and D. Trajkovic for in situ hybridization and histological assistance, B. Webb and G. Siuzdak for assistance with mass spectrometry, K. Spencer for confocal microscopy assistance, W. Balch and M. McHeyzer-Williams for use of equipment, B. Pham and D. Chiu for slide preparation, members of the Chun lab for discussions and support, D. Letourneau for editorial assistance, S. Liu for supplying a custom syringe for injections, and Kirin Brewery for providing Ki16425. **Funding:** This work was supported by NIH grants MH051699 and NS048478, Scripps Translational Science Initiative grant U54 RR025774 (J.C.), and an NSF predoctoral fellowship (Y.C.Y.). Y.C.Y. is currently a Hydrocephalus Association Mentored Young Investigator. **Author contributions:** Y.C.Y. and J.C. designed the research; Y.C.Y. performed head size measurements and in situ hybridizations; Y.C.Y. and T.M. performed in vivo experiments; M.-E.L. optimized and prepared lipid extracts for LC-MS; Y.C.Y. and K.N. quantified Rac and Rho GTPases; R.R.R. generated the receptor-null animals; Y.C.Y., J.W.C., and M.A.K. quantified mitotic cell displacement and ventricular size; Y.C.Y. performed data analysis; and Y.C.Y. and J.C. wrote the paper. **Competing interests:** J.C. is a scientific advisory board member for Amira Pharmaceuticals. The other authors declare that they have no competing interests.

Submitted 29 December 2010

Accepted 18 August 2011

Published 7 September 2011

10.1126/scitranslmed.3002095

Citation: Y. C. Yung, T. Mutoh, M.-E. Lin, K. Noguchi, R. R. Rivera, J. W. Choi, M. A. Kingsbury, J. Chun, Lysophosphatidic acid signaling may initiate fetal hydrocephalus. *Sci. Transl. Med.* **3**, 99ra87 (2011).